Quantum-tunneling rates and stationary solutions in dispersive optical bistability

K. Vogel and H. Risken
Abteilung für Theoretische Physik, Universität Ulm, D-7900 Ulm, Federal Republic of Germany
(Received 22 February 1988)

For the model of Drummond and Walls describing dispersive optical bistability, stationary solutions as well as quantum-tunneling rates are calculated by solving a pseudo-Fokker-Planck equation (PFPE), i.e., a Fokker-Planck-like equation with a non-positive-definite diffusion matrix, in terms of matrix continued fractions. Due to the quantum nature of the model, an interesting oscillating variation of the decay rates of the PFPE as a function of the scaling factor for the photon number is found for small cavity damping.

I. INTRODUCTION

In the past decade optical bistability has become an important field in quantum optics (see, for instance, Refs. 1–4 for reviews). In optical bistability, as in every bistable system, there are two stable states. Without any fluctuations the system stays in one of these two stable states. If fluctuations are taken into account, one has a certain probability that the system jumps from one state to the other. Obviously, an appreciable jumping rate would destroy the usefulness of an optical bistable device. Therefore one tries to eliminate these fluctuations. In principle this is possible for external as well as for thermal fluctuations. Quantum fluctuations, however, cannot be eliminated. These quantum fluctuations also lead to transitions from one state to the other. In this case one talks of quantum tunneling in analogy to the quantum motion of a particle in a double-well potential. Because a potential does not exist for dispersive optical bistability this is, however, only a formal analogy. In the present paper our main objective is the determination of these quantum-tunneling rates for the model of Drummond and Walls[5] describing dispersive optical bistability. These quantum-tunneling rates are very important because they determine the ultimate stability of the two stable states, i.e., they determine the ultimate limits of working conditions for such a device. (For absorptive optical bistability Savage and Walls[6] suggested to reduce the tunneling rate by using a squeezed vacuum field as cavity input.)

In the model of Drummond and Walls[5] a single quantized field mode inside the cavity is driven by an external coherent classical field. The nonlinear material inside the cavity is described by a nonlinear polarization. Dissipation due to cavity losses is taken into account by a coupling to a heat bath, as usually done in quantum optics. The model has the advantage that only the operator for the cavity light mode enter in the equation of motion for the density operator. Besides this simplicity it is a nonlinear and nontrivial quantum model fully capable of describing the quantum fluctuations. In addition to quantum fluctuations, thermal fluctuations are also included in the model. Solutions of this master equation have been derived for the following two cases. (1) Analytical results for stationary expectation values of the field operator in the absence of thermal fluctuations have been derived in Ref. 5 by using the complex P function of Gardiner.[7–9] In addition to these solutions, nonstationary solutions have been obtained in Ref. 5 by a linearization procedure. (Such a linearization, however, does not lead to the tunneling rate.) (2) In the low-damping limit tunneling rates, i.e., the lowest nonzero eigenvalues of the master equation for the density operator, have been obtained numerically in Ref. 10 by solving an appropriate Pauli-type master equation. Stationary Q functions as well as expectation values are also calculated in that reference.

In order to solve the equation of motion for the density operator we derive an equation of motion for the Glauber-Sudarshan P function[11,12] and for the Q function, i.e., for the expectation value of the density operator with respect to a coherent state. An equation of motion for the Wigner distribution[13] is also obtained. (For a review of different representations of the density operator see Ref. 14.) It turns out that the equations of motion for the P and the Q function have the form of a Fokker-Planck equation, but the diffusion matrix is not positive definite or semidefinite. Therefore it is not an ordinary Fokker-Planck equation (FPE) and it cannot be interpreted as describing the Brownian motion of a particle under the influence of a suitable force. For this reason we termed such an equation a pseudo-Fokker-Planck equation (PFPE). (Fokker-Planck equations with non-positive-definite diffusion matrices are also treated in Refs. 15 and 16. These PFPE's have linear drift coefficients and are therefore much easier to handle than the present one.)

By doubling the phase space and introducing the positive P function, it is possible to derive a Fokker-Planck equation with a positive definite or positive semidefinite diffusion matrix. (For a discussion of generalized representations of the density operator the reader is referred to Refs. 7–9 and 17.) The Langevin equations corresponding to the Fokker-Planck equation can then be simulated,[18] but one has to handle twice as many variables as in the original problem.

For a non-positive-definite diffusion matrix we may still have a stable stationary and time-dependent solution. A simple illustrative example is given in the Appendix.

Therefore we use for our calculations the equations of motion for the P and Q function with their non-positive-definite diffusion matrices instead of the Fokker-Planck equation for the positive P function. By applying the matrix continued-fraction (MCF) method, which was developed in Ref. 19 (see also Ref. 20 for a review) for solving two-variable FPE's, we obtain the stationary solution as well as the lowest nonzero eigenvalue and some of the low real eigenvalues of the PFPE for the Q function. It turns out that in the bistable region the lowest nonzero eigenvalue is well separated from the higher ones and therefore determines the decay rate of the stable states, i.e., the tunneling rate. Additionally, we show that, due to the quantum nature of the problem, the tunneling rates show an interesting oscillating variation as a function of a system parameter by which the photon number inside the cavity scales. The main idea of this procedure and preliminary results are reported in Refs. 21–23.

The present paper is organized as follows. In Sec. II we present the model and the basic equations. In Sec. III the pseudo-Fokker-Planck equation is given. Next, in Sec. IV we show by a suitable expansion of the P and Q function how the PFPE can be reduced to a tridiagonal vector recurrence relation. In Sec. V we explain the matrix continued fraction (MCF) method for solving the tridiagonal vector recurrence relation. Finally, in Sec. VI the results for the stationary solution as well as for the eigenvalues are presented.

II. MODEL AND BASIC EQUATIONS

In their model for dispersive optical bistability, Drummond and Walls[5] consider a single-mode field inside a cavity which contains a nonlinear dispersive medium. The mode is driven by an external classical coherent driving field. In their derivation of the master equation the polarization is introduced phenomenologically and it is expanded up to third order. By neglecting the second-order term in this expansion and using the rotating-wave approximation they obtained a single-mode Hamiltonian of the form

$$H/\hbar=\omega_c a^\dagger a+\chi a^{\dagger 2}a^2 , \tag{2.1}$$

where ω_c is the frequency of the cavity mode and χ is the anharmonicity parameter. Adding the Hamiltonian for the coherent driving field with frequency ω_L and including a loss mechanism, which takes into account the cavity damping, they derived a master equation for the density operator of the cavity field mode. In a reference frame rotating at frequency ω_L and in a slightly different notation this master equation can be written as

$$\dot{\rho}=-i[H/\hbar,\rho]+\kappa L_{\rm ir}[\rho] , \tag{2.2}$$

where $H/\hbar$ and $L_{\rm ir}[\rho]$ are given by

$$H/\hbar=-\Omega a^\dagger a+\chi a^{\dagger 2}a^2-F(a+a^\dagger) , \tag{2.3}$$

$$L_{\rm ir}[\rho]=2a\rho a^\dagger-\rho a^\dagger a-a^\dagger a\rho+2n_{\rm th}[[a,\rho],a^\dagger] . \tag{2.4}$$

Here Ω is the difference between the frequency of the driving field and the frequency of the cavity mode, i.e., $\Omega=\omega_L-\omega_c$; F is the amplitude of the driving field in suitable units, which can be chosen to be real; κ is the cavity damping constant; $n_{\rm th}$ is the number of thermal photons inside the cavity; and $a^\dagger$ and a are the creation and annihilation operators for the light field inside the cavity.

In Ref. 24 a microscopic model of optical bistability, taking into account the microscopic nature of the medium inside the cavity, was investigated. The medium was treated as a two-level system and it was assumed that a large number of atoms are present. After deriving an equation of motion for the positive P function containing both the field variables and the atomic variables and after adiabatically eliminating the atomic variables, Drummond and Walls obtained an equation of motion for the positive P function containing only the field variables. In the dispersive limit and if our notation is used this equation agrees with the equation of motion for the P function, which we will obtain from (2.2) in Sec. III. By performing the adiabatic elimination and taking the dispersive limit, the model based on the Hamiltonian (2.1) can then be put on a microscopic basis. In contrast to Ref. 24 where a large number of atoms was considered, Savage and Carmichael[25] have shown that absorptive optical bistability may exist even for a single two-level-atom system.

A. Classical limit

From (2.2) one obtains for the expectation value of the operators a and $a^\dagger$,

$$\alpha=\mathrm{Tr}(a\rho),\quad \alpha^*=\mathrm{Tr}(a^\dagger\rho) , \tag{2.5}$$

the following equation:

$$\dot{\alpha}=i\Omega\alpha-\kappa\alpha-2i\chi\mathrm{Tr}(a^\dagger a^2\rho)+iF . \tag{2.6}$$

By factorizing the term $\mathrm{Tr}(a^\dagger a^2\rho)$ we arrive at the "classical" equation without fluctuations (see also Refs. 5 and 10),

$$\dot{\alpha}=(i\Omega-\kappa-2i\chi|\alpha|^2)\alpha+iF . \tag{2.7}$$

It should be mentioned that the factorization is a good approximation in the limit $\Omega/\chi\to\infty$, i.e., for a large number of photons inside the cavity; see below. Only in this limit can the factorization be performed uniquely. Introducing the normalized quantities ($\Omega>0$, otherwise the system is not bistable for any value of the driving field F)

$$\tilde{t}=\Omega t,\quad \tilde{\alpha}=\sqrt{\chi/\Omega}\alpha,\quad \tilde{I}=\frac{\chi}{\Omega}\alpha^*\alpha ,$$
$$\tilde{\kappa}=\kappa/\Omega,\quad \tilde{F}=\frac{1}{\Omega}\sqrt{\chi/\Omega}F , \tag{2.8}$$

Eq. (2.7) is transformed into the normalized form

$$\frac{d\tilde{\alpha}}{d\tilde{t}}=[i(1-2|\tilde{\alpha}|^2)-\tilde{\kappa}]\tilde{\alpha}+i\tilde{F} . \tag{2.9}$$

The unnormalized intensity $I=\alpha^*\alpha=\mathrm{Tr}(a^\dagger a\rho)$ is the photon number inside the cavity. Because I scales with Ω/χ, this parameter essentially describes the number of photons inside the cavity ($\tilde{I}$ is of the order 1; see Fig. 1).

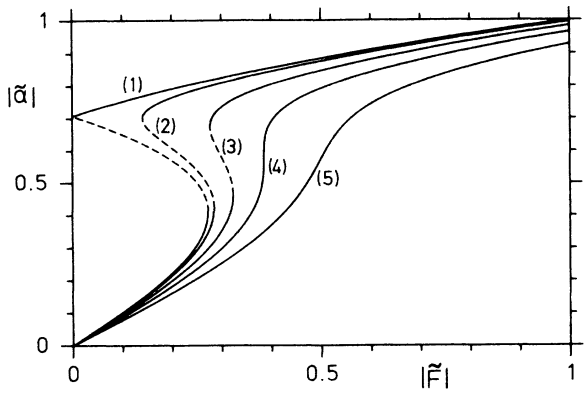

FIG. 1. Stable (solid lines) and unstable (dashed lines) stationary solutions of (2.9) as a function of the scaled driving field $|\tilde{F}|$ for (1) $\tilde{\kappa}=0$, (2) $\tilde{\kappa}=0.2$, (3) $\tilde{\kappa}=0.4$, (4) $\tilde{\kappa}=1/\sqrt{3}$, and (5) $\tilde{\kappa}=0.8$.

For the stationary state (i.e., $d\tilde{\alpha}/d\tilde{t}=0$) the following relation between the driving field $\tilde{F}$ and the intensity $\tilde{I}$ can be derived:

$$|\tilde{F}|=\{\tilde{I}[\tilde{\kappa}^2+(1-2\tilde{I})^2]\}^{1/2} . \tag{2.10}$$

It follows from a linearization procedure around the stationary solution of (2.9) that the solution is stable for $d|F|/d\tilde{I}>0$, whereas it is unstable for $d|\tilde{F}|/d\tilde{I}<0$. If the damping constant is small enough, i.e.,

$$\tilde{\kappa}<1/\sqrt{3} , \tag{2.11}$$

there are two stable and one unstable stationary solutions for $|\tilde{F}|$ in the range

$$[1+9\tilde{\kappa}^2-(1-3\tilde{\kappa}^2)^{3/2}]^{1/2} < 3\sqrt{3}|\tilde{F}| < [1+9\tilde{\kappa}^2+(1-3\tilde{\kappa}^2)^{3/2}]^{1/2} , \tag{2.12}$$

otherwise, i.e., either for $\tilde{\kappa}>1/\sqrt{3}$ or for $|\tilde{F}|$ outside the interval (2.12), there is only one stable solution; see Fig. 1.

B. Connection to the Duffing equation

The classical equation (2.7) is the rotating-wave approximation of the driven Duffing oscillator equation,[26,27] i.e., an oscillator equation where the frequency depends on the amplitude,

$$\ddot{E}+2\kappa\dot{E}+\omega_c^2\left[1+\frac{4\chi}{3\omega_c}E^2\right]E=4\omega_L F\cos\omega_L t . \tag{2.13}$$

To derive the rotating-wave approximation of (2.13) one inserts

$$E(t)=\alpha(t)\exp(-i\omega_L t)+\text{c.c.}$$

into (2.13). Neglecting the second-order derivative of the slowly varying amplitude $\alpha(t)$ and using $\kappa|\dot{\alpha}|\ll\omega_c^2|\alpha|$ one obtains (2.7). From the Duffing equation the low and high intensity solution in Fig. 1 are easily explained. If we start with a low intensity $I\sim E^2$ the frequency of the oscillator is ω_c and it differs from the driving frequency ω_L. Because of this mismatch the amplitude remains small and the stationary solution is on the low-intensity branch. If we start with an intensity such that $\omega_c^2[1+4\chi E^2/(3\omega_c)]\approx\omega_L^2$, i.e., the frequency of the oscillator approximately equals the frequency of the driving force, this resonance effect then leads to a large amplitude and the stationary solution is on the high-intensity branch.

III. PSEUDO-FOKKER-PLANCK EQUATION

Any normally or antinormally ordered expectation value of the light-field operators a and $a^\dagger$ may be obtained from both characteristic functions

$$\tilde{P}(\beta)=\tilde{P}^{+}(\beta)=\mathrm{Tr}(e^{i\beta^* a^\dagger}e^{i\beta a}\rho) , \tag{3.1a}$$

$$\tilde{Q}(\beta)=\tilde{P}^{-}(\beta)=\mathrm{Tr}(e^{i\beta a}e^{i\beta^* a^\dagger}\rho) , \tag{3.1b}$$

by appropriate differentiation with respect to β and β^*. Furthermore, one may define a third characteristic function

$$\tilde{W}(\beta)=\mathrm{Tr}(e^{i\beta^* a^\dagger+i\beta a}\rho) . \tag{3.2}$$

Due to the operator relation

$$e^{A+B}=e^{A}e^{B}e^{-[A,B]/2}$$

$$\text{for } [[A,B],A]=[[A,B],B]=0 , \tag{3.3}$$

the three characteristic functions (3.1a), (3.1b), and (3.2) differ only by factors:

$$\tilde{Q}(\beta)=e^{-|\beta|^2/2}\tilde{W}(\beta)=e^{-|\beta|^2}\tilde{P}(\beta) . \tag{3.4}$$

The Fourier transforms of these characteristic functions,

$$P^{\pm}(\alpha)=\frac{1}{\pi^2}\int e^{-i\alpha\beta-i\alpha^*\beta^*}\tilde{P}^{\pm}(\beta)d^2\beta , \tag{3.5}$$

$$W(\alpha)=\frac{1}{\pi^2}\int e^{-i\alpha\beta-i\alpha^*\beta^*}\tilde{W}(\beta)d^2\beta , \tag{3.6}$$

are the Glauber-Sudarshan P function ($P\equiv P^+$), the Q function ($Q\equiv P^-$), and the Wigner distribution W; see, for instance, Refs. 14, 28, and 29. Because the equations of motion for the P and Q function differ only by $\pm$ signs [see (3.12)], we have introduced the notation

$$P(\alpha)=P^{+}(\alpha),\quad Q(\alpha)=P^{-}(\alpha) . \tag{3.7}$$

The Q function can be expressed in terms of the density operator according to

$$Q(\alpha)=P^{-}(\alpha)=\langle\alpha|\rho|\alpha\rangle/\pi,\quad |\alpha\rangle=\text{coherent state} \tag{3.8}$$

whereas the density operator itself can be expressed by the Glauber-Sudarshan P function according to

$$\rho=\int|\alpha\rangle\langle\alpha|P(\alpha)d^2\alpha . \tag{3.9}$$

Normally and antinormally ordered expectation values are obtained from the P and Q function by integration,

$$\langle a^{\dagger n}a^m\rangle=\int\alpha^{*n}\alpha^m P(\alpha)d^2\alpha , \tag{3.10}$$

$$\langle a^m a^{\dagger n}\rangle = \int \alpha^m \alpha^{*n} Q(\alpha) d^2\alpha \ . \tag{3.11}$$

For squeezed states the P function does not exist in general. (For a discussion of squeezed states see, for instance, Ref. 30.) Nevertheless, the expansion coefficients of the P function into a complete set of functions do exist because they are connected with the expectation values. Therefore the equations of motion for the coefficients of the P function may also be used for calculating expectation values and eigenvalues, see Secs. IV and V.

By standard techniques (see, for instance, Refs. 9, 28, and 29) the operator master equation (2.2) is transformed into an equation of motion for the P function, the Q function, and the Wigner distribution. These partial differential equations read

$$\begin{aligned}\frac{\partial P^{\pm}}{\partial t} = &-\frac{\partial}{\partial\alpha}[-\kappa\alpha + i\Omega\alpha + 2i(1\mp 1)\chi\alpha - 2i\chi\alpha^2\alpha^* + iF]P^{\pm} \\ &-\frac{\partial}{\partial\alpha^*}[-\kappa\alpha^* - i\Omega\alpha^* - 2i(1\mp 1)\chi\alpha^* + 2i\chi\alpha^{*2}\alpha - iF]P^{\pm} \\ &\mp i\chi\frac{\partial^2}{\partial\alpha^2}\alpha^2 P^{\pm} + 2\kappa(n_{\rm th}+\tfrac{1}{2}\mp\tfrac{1}{2})\frac{\partial^2 P^{\pm}}{\partial\alpha^*\partial\alpha} \pm i\chi\frac{\partial^2}{\partial\alpha^{*2}}\alpha^{*2}P^{\pm} \ ,\end{aligned} \tag{3.12}$$

$$\begin{aligned}\frac{\partial W}{\partial t} = &-\frac{\partial}{\partial\alpha}(-\kappa\alpha + i\Omega\alpha + 2i\chi\alpha - 2i\chi\alpha^2\alpha^* + iF)W - \frac{\partial}{\partial\alpha^*}(-\kappa\alpha^* - i\Omega\alpha^* - 2i\chi\alpha^* + 2i\chi\alpha^{*2}\alpha - iF)W \\ &+2\kappa(n_{\rm th}+\tfrac{1}{2})\frac{\partial^2 W}{\partial\alpha^*\partial\alpha} + \frac{i}{2}\chi\left(\frac{\partial^3}{\partial\alpha\,\partial\alpha^{*2}}\alpha^* - \frac{\partial^3}{\partial\alpha^*\partial\alpha^2}\alpha\right)W \ .\end{aligned} \tag{3.13}$$

In (3.12) the upper signs are valid for the P function, while the lower signs are valid for the Q function. The equation of motion for the P function is also easily obtained from the equation of motion for the generalized P representation derived in Ref. 5 by setting $\alpha^{\dagger}=\alpha^*$ and using our notation. Comparing (3.12) and (3.13) one realizes that the terms containing first-order derivatives differ only by the terms $2i\chi\alpha$ and $2i\chi\alpha^*$, whereas the second-order-derivative terms in (3.12) are replaced by second- and third-order derivatives. It should be noted that in (3.13) the third-order-derivative terms are due to the nonlinearity in the Hamiltonian (2.1). Because of the special form of the Hamiltonian (2.1), Eq. (3.12) does not contain higher than second-order derivatives. Other nonlinearities such as a^4 or $a^{\dagger 3}a^3$ would yield higher-order derivatives. The terms stemming from the loss mechanism are quite similar for all three functions P, Q, and W,

$$\kappa\left(\frac{\partial}{\partial\alpha}\alpha + \frac{\partial}{\partial\alpha^*}\alpha^* + 2(n_{\rm th}+f)\frac{\partial^2}{\partial\alpha^*\partial\alpha}\right)\begin{Bmatrix}P\\W\\Q\end{Bmatrix}, \tag{3.14}$$

$$f = \begin{cases}0 & \text{for the } P \text{ function}\\ \frac{1}{2} & \text{for the Wigner distribution}\\ 1 & \text{for the } Q \text{ function} \ .\end{cases}$$

Although third-order or higher-order derivatives can also be handled by the MCF method, we investigate in the present paper only the pseudo-Fokker-Planck equation for the P and the Q function because it has a simpler form than the equation of motion for the Wigner distribution. It should be noted, however, that the results obtained from the Wigner distribution should agree with the results obtained via the P and Q function because the representations (3.12) and (3.13) of the master equation (2.2) are equivalent and no further simplification or approximation will be made. As shown in Sec. VI the results obtained from either the P or the Q function do agree. This is in contrast to the problem of representation-dependent tunneling times discussed in Ref. 31, where a model for absorptive optical bistability was investigated. In this reference equations of motions for different representations have been derived. Each of these representations contains higher than second-order derivatives. If phase diffusion is neglected and the equations are truncated after the second-order derivatives, approximate results for the tunneling times can be obtained. These results depend on the representation and can differ by orders of magnitude, as shown in Ref. 31.

In the real notation

$$\begin{aligned}&\alpha = \alpha_1 + i\alpha_2 \ ,\\ &\frac{\partial}{\partial\alpha} = \frac{1}{2}\left(\frac{\partial}{\partial\alpha_1} - i\frac{\partial}{\partial\alpha_2}\right) \ ,\\ &\frac{\partial}{\partial\alpha^*} = \frac{1}{2}\left(\frac{\partial}{\partial\alpha_1} + i\frac{\partial}{\partial\alpha_2}\right) \ ,\end{aligned} \tag{3.15}$$

(3.12) takes the form (summation convention for repeated indices)

$$\frac{\partial P^{\pm}}{\partial t} = -\frac{\partial}{\partial\alpha_i}D_i^{\pm}P^{\pm} + \frac{\partial}{\partial\alpha_i}\frac{\partial}{\partial\alpha_j}D_{ij}^{\pm}P^{\pm} \ , \tag{3.16}$$

where the drift and diffusion coefficients are given by

$$\begin{aligned}D_1^{\pm} &= -\kappa\alpha_1 - \Omega\alpha_2 - 2(1\mp 1)\chi\alpha_2 + 2\chi\alpha_2(\alpha_1^2+\alpha_2^2) \ ,\\ D_2^{\pm} &= -\kappa\alpha_2 + \Omega\alpha_1 + 2(1\mp 1)\chi\alpha_1 - 2\chi\alpha_1(\alpha_1^2+\alpha_2^2) + F \ ,\\ D_{11}^{\pm} &= \pm\chi\alpha_1\alpha_2 + \frac{\kappa}{2}(n_{\rm th}+\tfrac{1}{2}\mp\tfrac{1}{2}) \ ,\\ D_{12}^{\pm} &= D_{21}^{\pm} = \mp\frac{\chi}{2}(\alpha_1^2-\alpha_2^2) \ ,\\ D_{22}^{\pm} &= \mp\chi\alpha_1\alpha_2 + \frac{\kappa}{2}(n_{\rm th}+\tfrac{1}{2}\mp\tfrac{1}{2}) \ .\end{aligned} \tag{3.17}$$

It is easily derived from (3.17) that the diffusion matrix $D_{ij}^{\pm}$ is not positive definite or semidefinite if the intensity is large enough, i.e.,

$$D_{11}^{\pm}D_{22}^{\pm}-(D_{12}^{\pm})^2<0$$

$$\text{for } \alpha^*\alpha=\alpha_1^2+\alpha_2^2>\frac{\kappa}{\chi}(n_{\text{th}}+\tfrac{1}{2}\mp\tfrac{1}{2}) . \quad (3.18)$$

Because the diffusion matrix is not positive definite or positive semidefinite everywhere, (3.16) and (3.17) cannot be interpreted as a Fokker-Planck equation describing the Brownian motion under the influence of a suitable force. For this reason we termed (3.16) and (3.17) a pseudo-Fokker-Planck equation. One may argue that equations of this type are unphysical and cannot be solved because the solution will become singular due to the non-positive-definite diffusion matrix. In the Appendix, however, we show for a simple equation with a non-positive-definite diffusion matrix that such an equation can have nonsingular solutions. As we will see in Sec. VI, nonsingular solutions of (3.12) can be obtained for the Q function.

A Fokker-Planck equation derived from an arbitrary Langevin equation always has a positive or positive semidefinite diffusion matrix. Therefore a Langevin equation leading to (3.16) and (3.17) does not exist and thus (3.16) and (3.17) cannot be investigated by digital or analog simulation methods. However, by doubling the phase space it is possible to introduce a generalized P representation—the positive P representation .[7-9,17] The equation of motion for this positive P representation is a Fokker-Planck equation with a positive or positive semidefinite diffusion matrix. From this Fokker-Planck equation one may then obtain a Langevin equation which can be solved by simulations.[18] Instead of *two* real variables one now has to handle *four* real variables. Furthermore, the tunneling times, which we calculate with the MCF method, may become very small (see Sec. VI) and it is difficult to determine them by simulations. Therefore the complex P representation used in Ref. 5 and the positive P representation seems to be useful for analytical calculations, while the positive P representation must be used for simulations. For a direct numerical solution, however, the Q function is more useful because only *two* real variables have to be taken into account. For simulation methods another problem arises if the equation of motion for the P function contains higher than second-order derivatives. Then the equation of motion for the positive P representation also contains higher-order derivatives and does not have the form of a Fokker-Planck equation. In this case no simulations are possible because a Langevin equation does not exist. As already mentioned in principle, the MCF method can still be applied to such problems.

A. Classical limit of the pseudo-Fokker-Planck equation

Using the normalized quantities (2.8), Eq. (3.12) can be written as

$$\frac{\partial\tilde{P}^{\pm}}{\partial\tilde{t}}=-\frac{\partial}{\partial\tilde{\alpha}}\left[-\tilde{\kappa}\tilde{\alpha}+i\tilde{\alpha}+2i\frac{\chi}{\Omega}(1\mp1)\tilde{\alpha}-2i\tilde{\alpha}^2\tilde{\alpha}^*+i\tilde{F}\right]\tilde{P}^{\pm}-\frac{\partial}{\partial\tilde{\alpha}^*}\left[-\tilde{\kappa}\tilde{\alpha}^*-i\tilde{\alpha}^*-2i\frac{\chi}{\Omega}(1\mp1)\tilde{\alpha}^*+2i\tilde{\alpha}^{*2}\tilde{\alpha}-i\tilde{F}\right]\tilde{P}^{\pm}$$
$$\mp i\frac{\chi}{\Omega}\frac{\partial^2}{\partial\tilde{\alpha}^2}\tilde{\alpha}^2\tilde{P}^{\pm}+2\tilde{\kappa}\frac{\chi}{\Omega}(n_{\text{th}}+\tfrac{1}{2}\mp\tfrac{1}{2})\frac{\partial^2\tilde{P}^{\pm}}{\partial\tilde{\alpha}^*\partial\tilde{\alpha}}\pm i\frac{\chi}{\Omega}\frac{\partial^2}{\partial\tilde{\alpha}^{*2}}\tilde{\alpha}^{*2}\tilde{P}^{\pm} . \quad (3.19)$$

In the limit $\chi/\Omega\to0$, $n_{\text{th}}\chi/\Omega\to\text{const}=2D/\tilde{\kappa}$, (3.19) reduces to

$$\frac{\partial\tilde{P}}{\partial\tilde{t}}=-\frac{\partial}{\partial\tilde{\alpha}}(-\tilde{\kappa}\tilde{\alpha}+i\tilde{\alpha}-2i\tilde{\alpha}^2\tilde{\alpha}^*+i\tilde{F})\tilde{P}$$
$$-\frac{\partial}{\partial\tilde{\alpha}^*}(-\tilde{\kappa}\tilde{\alpha}^*-i\tilde{\alpha}^*+2i\tilde{\alpha}^{*2}\tilde{\alpha}-i\tilde{F})\tilde{P}$$
$$+4D\frac{\partial^2\tilde{P}}{\partial\tilde{\alpha}^*\partial\tilde{\alpha}} . \quad (3.20)$$

Because the equations for both the P and the Q function agree in the preceding limit the distinction between the P and the Q function is no longer necessary. [By performing the same procedure for the Wigner distribution we also obtain (3.20).] Equation (3.20) is just the Fokker-Planck equation which is obtained by adding complex Gaussian white noise $\Gamma(t)$ of the form

$$\langle\Gamma(t)\rangle=\langle\Gamma^*(t)\rangle$$
$$=\langle\Gamma(t)\Gamma(t')\rangle=\langle\Gamma^*(t)\Gamma^*(t')\rangle=0 ,$$
$$\langle\Gamma(t)\Gamma^*(t')\rangle=\langle\Gamma^*(t)\Gamma(t')\rangle=4D\delta(t-t') , \quad (3.21)$$

to (2.9). Graham and Schenzle[32] and Haug *et al.*[33] already obtained a Fokker-Planck equation similar to (3.20) by starting from classical equations and adding white noise.

IV. EXPANSION IN COMPLETE SET AND DERIVATION OF VECTOR RECURRENCE RELATIONS

For numerical calculations it seems to be more appropriate to use the intensity I and the phase ϕ defined by

$$\alpha=\sqrt{I}e^{i\phi} \quad (4.1)$$

instead of the complex amplitude α. Equation (3.12) is then transformed to the following pseudo-Fokker-Planck equation in the variables I and ϕ,

$$\frac{\partial P^{\pm}}{\partial t}=\left[-\frac{\partial}{\partial I}[-2\kappa I+\kappa(2n_{\text{th}}+1\mp1)+2F\sqrt{I}\sin\phi]\right.$$
$$-\frac{\partial}{\partial\phi}\left[\Omega-2\chi(I-1)\mp\chi+\frac{F}{\sqrt{I}}\cos\phi\right]$$
$$+\kappa(2n_{\text{th}}+1\mp1)\frac{\partial^2}{\partial I^2}I\mp2\chi\frac{\partial^2}{\partial I\,\partial\phi}I$$
$$\left.+\frac{\kappa}{4I}(2n_{\text{th}}+1\mp1)\frac{\partial^2}{\partial\phi^2}\right]P^{\pm} . \quad (4.2)$$

For treating (4.2) numerically $P^{\pm}$ is expanded into two complete sets of functions. Since $P^{\pm}(I,\phi,t)$ is periodic in ϕ with period 2π and the variable I is defined only for $I \geq 0$, we expand $P^{\pm}$ into a Fourier series with respect to ϕ and into Laguerre functions with respect to I according to

$$P^{\pm}(I,\phi,t)=\sum_{m=0}^{\infty}\left[a_m^0 e^{-I/I_s}L_m^0(I/I_s)+\sum_{n=1}^{\infty}\frac{2}{\sqrt{n!}}[a_m^n\cos(n\phi)-b_m^n\sin(n\phi)]\times e^{-I/I_s}(I/I_s)^{n/2}\times L_m^n(I/I_s)\right]. \tag{4.3}$$

Here L_m^n are the generalized Laguerre polynomials[34] and I_s is an arbitrary scaling intensity which can be chosen in such a way that good numerical convergence is achieved. The factor $1/\sqrt{n!}$ was added in order to reduce the numerical errors for the matrix inversions which occur in the MCF's in Sec. V. The terms $(I/I_s)^{n/2}$ follow from the asymptotic behavior for $I\to 0$. An expansion of this type was already used in Refs. 33 and 35. Substituting the series (4.3) into (4.2), using some recurrence relations for Laguerre polynomials,[34] and using the orthogonality relation

$$\frac{m!}{\Gamma(n+m+1)}\int_0^{\infty}e^{-x}x^n L_m^n(x)L_{m'}^n(x)dx=\delta_{mm'}, \tag{4.4}$$

the following expression for the time-dependent expansion coefficients $a_m^n(t)$ and $b_m^n(t)$ can be derived after some algebra ($n\geq 1$, $m\geq 0$, and coefficients with a negative lower index formally occurring for $m=0$ can be omitted because of the prefactor m),

$$\begin{aligned}
\dot{a}_m^0 &= \frac{2Fm}{\sqrt{I_s}}b_{m-1}^1-\frac{2\kappa}{I_s}(n_{\rm th}+\tfrac{1}{2}\mp\tfrac{1}{2}-I_s)ma_{m-1}^0-2\kappa m a_m^0,\\
\dot{a}_m^n &= \frac{Fm}{\sqrt{(n+1)I_s}}b_{m-1}^{n+1}+F\sqrt{n/I_s}\,b_m^{n-1}-\frac{2\kappa}{I_s}(n_{\rm th}+\tfrac{1}{2}\mp\tfrac{1}{2}-I_s)ma_{m-1}^n\\
&\quad -\kappa(2m+n)a_m^n-n[(2I_s\pm 1)(2m+n+1)\chi-2\chi-\Omega]b_m^n+2nm\chi(I_s\pm 1)b_{m-1}^n+2\chi I_s n(n+m+1)b_{m+1}^n,\quad n\geq 1\\
\dot{b}_m^n &= -\frac{Fm}{\sqrt{(n+1)I_s}}a_{m-1}^{n+1}-F\sqrt{n/I_s}\,a_m^{n-1}-\frac{2\kappa}{I_s}(n_{\rm th}+\tfrac{1}{2}\mp\tfrac{1}{2}-I_s)mb_{m-1}^n\\
&\quad -\kappa(2m+n)b_m^n+n[(2I_s\pm 1)(2m+n+1)\chi-2\chi-\Omega]a_m^n-2nm\chi(I_s\pm 1)a_{m-1}^n-2\chi I_s n(n+m+1)a_{m+1}^n,\quad n\geq 1.
\end{aligned} \tag{4.5}$$

In the last equation the upper sign is valid for the expansion coefficients of the P function and the lower sign is valid for the expansion coefficient of the Q function. Defining the vectors $\mathbf{c}_m$ by

$$\mathbf{c}_m=(a_m^0,a_m^1,b_m^1,a_m^2,b_m^2,\ldots), \tag{4.9}$$

the recurrence relation (4.5) can be written in the tridiagonal form

$$\dot{\mathbf{c}}_m=\mathbf{Q}_m^{+}\mathbf{c}_{m+1}+\mathbf{Q}_m\mathbf{c}_m+\mathbf{Q}_m^{-}\mathbf{c}_{m-1}, \tag{4.10}$$

where the matrices $\mathbf{Q}_m^{+}$, $\mathbf{Q}_m$, and $\mathbf{Q}_m^{-}$ are defined by

$$\begin{aligned}
(\mathbf{Q}_m^{+})_{n,n'} &= -I_s\chi n\left[m+\frac{n}{2}+1\right]\delta_{n,n'+1}\quad (n\ \text{even}),\\
(\mathbf{Q}_m^{+})_{n,n'} &= +I_s\chi(n+1)\left[m+\frac{n+1}{2}+1\right]\delta_{n,n'-1}\quad (n\ \text{odd}),
\end{aligned} \tag{4.11a}$$

$$\begin{aligned}
(\mathbf{Q}_m)_{n,0} &= -2\kappa m\delta_{n,0}-F/\sqrt{I_s}\,\delta_{n,2},\\
(\mathbf{Q}_m)_{n,n'} &= -\frac{n+1}{2}\chi\left[(2I_s\pm 1)\left[2m+\frac{n+1}{2}+1\right]-\frac{\Omega}{\chi}-2\right]\delta_{n,n'-1}-\kappa\left[2m+\frac{n+1}{2}\right]\delta_{n,n'}\\
&\quad +F\left[\frac{n+1}{2I_s}\right]^{1/2}\delta_{n,n'+1}\quad (n\ \text{odd},\ n'\geq 1),
\end{aligned} \tag{4.11b}$$

The normalization

$$\int P(\alpha,t)d^2\alpha=\int Q(\alpha,t)d^2\alpha=\int P^{\pm}(\alpha,t)d^2\alpha=1 \tag{4.6}$$

requires

$$a_0^0(t)=1/\pi I_s \tag{4.7}$$

for the expansion of the P and the Q function. Higher-order expansion coefficients are connected with the moments. We have, for instance,

$$\begin{aligned}
\langle a\rangle &= \pi I_s^{3/2}(a_0^1-ib_0^1),\\
\langle a^{\dagger}a\rangle &= \pi I_s^2(a_0^0-a_1^0)-\tfrac{1}{2}\pm\tfrac{1}{2}.
\end{aligned} \tag{4.8}$$

$$(\mathbf{Q}_m)_{n,n'}=-\kappa\left[2m+\frac{n}{2}\right]\delta_{n,n'}+\frac{n}{2}\chi\left[(2I_s\pm1)\left[2m+\frac{n}{2}+1\right]-\frac{\Omega}{\chi}-2\right]\delta_{n,n'+1}-F\left[\frac{n}{2I_s}\right]^{1/2}\delta_{n,n'+3}\quad(n\text{ even},\ n'\geq1)\ ,$$

$$(\mathbf{Q}_m^-)_{0,n'}=-2\kappa I_s^{-1}m\,(n_{\rm th}+\tfrac{1}{2}\mp\tfrac{1}{2}-I_s)\delta_{n',0}+2mF/\sqrt{I_s}\,\delta_{n',2}\ ,$$

$$(\mathbf{Q}_m^-)_{n,n'}=-2\kappa I_s^{-1}m\,(n_{\rm th}+\tfrac{1}{2}\mp\tfrac{1}{2}-I_s)\delta_{n,n'}+\chi m\,(n+1)(I_s\pm1)\delta_{n,n'-1}+Fm\left[\frac{2}{I_s(n+3)}\right]^{1/2}\delta_{n,n'-3}\quad(n\text{ odd})\ ,$$

$$(\mathbf{Q}_m^-)_{n,n'}=-\chi mn(I_s\pm1)\delta_{n,n'+1}-2\kappa I_s^{-1}m\,(n_{\rm th}+\tfrac{1}{2}\mp\tfrac{1}{2}-I_s)\delta_{n,n'}-Fm\left[\frac{2}{I_s(n+2)}\right]^{1/2}\delta_{n,n'-1}\quad(n\text{ even},\ n\geq2)\ . \tag{4.11c}$$

For the time-dependent equation (4.10) we make the ansatz

$$\mathbf{c}_m(t)=\hat{\mathbf{c}}_m e^{-\lambda t}\ , \tag{4.12}$$

which reduces (4.10) to the eigenvalue equation

$$\mathbf{Q}_m^+\hat{\mathbf{c}}_{m+1}+(\mathbf{Q}_m+\lambda\mathbf{I})\hat{\mathbf{c}}_m+\mathbf{Q}_m^-\hat{\mathbf{c}}_{m-1}=0\ , \tag{4.13}$$

where $\mathbf{I}$ denotes the identity matrix. This eigenvalue equation can then be solved by the matrix continued-fraction method (MCF method) described in Sec. V.

V. MATRIX CONTINUED-FRACTION METHOD

In order to handle (4.13) numerically the expansion (4.3) has to be truncated, i.e.,

$$a_m^n=0,\quad b_m^n=0\quad\text{for } n>N,\ m>M\ . \tag{5.1}$$

Here N and M have to be chosen large enough so that the final results do not change within the required accuracy if N and M are increased. For $\Omega/\chi\approx10$ (a typical value for this parameter in Sec. VI) $N\approx20$ and $M\approx120$ is sufficient to obtain results which are accurate within the width of the lines in the figures. Higher Ω/χ values require higher N's and M's, whereas for smaller Ω/χ values smaller N's and M's can be used. Moreover, we used double-precision arithmetic for our numerical calculations. Due to the truncation (5.1) the size of the matrices $\mathbf{Q}_m^\pm$ and $\mathbf{Q}_m$ is $(2N+1)\times(2N+1)$ and only the vectors $\mathbf{c}_0,\mathbf{c}_1,\ldots,\mathbf{c}_M$ are taken into account. In order to solve (4.13) we introduce the "ratio" matrices $\mathbf{S}_m$ defined by

$$\hat{\mathbf{c}}_m=\mathbf{S}_m\hat{\mathbf{c}}_{m-1}\ . \tag{5.2}$$

In solid-state physics similar matrices occur and are usually called transfer matrices; see, for instance, Chap. 8.5 of Ref. 36. The matrices $\mathbf{S}_m$ are used to eliminate the vectors $\hat{\mathbf{c}}_m$ in (4.13) iteratively. For $m\geq1$ we obtain

$$[\mathbf{Q}_m^+\mathbf{S}_{m+1}\mathbf{S}_m+(\mathbf{Q}_m+\lambda\mathbf{I})\mathbf{S}_m+\mathbf{Q}_m^-]\hat{\mathbf{c}}_{m-1}=0\ . \tag{5.3}$$

By choosing the matrices $\mathbf{S}_m$ such that the recurrence relation

$$\mathbf{S}_m=-(\mathbf{Q}_m+\lambda\mathbf{I}+\mathbf{Q}_m^+\mathbf{S}_{m+1})^{-1}\mathbf{Q}_m^- \tag{5.4}$$

holds, (5.3) is fulfilled for $m\geq1$. Iteration of (5.4) leads to a matrix continued fraction. If the matrix inversions are written by fraction lines

$$\mathbf{A}^{-1}=\frac{\mathbf{I}}{\mathbf{A}}\ ,$$

this MCF reads explicitly

$$\mathbf{S}_m=-\cfrac{\mathbf{I}}{\mathbf{Q}_m+\lambda\mathbf{I}-\mathbf{Q}_m^+\cfrac{\mathbf{I}}{\mathbf{Q}_{m+1}+\lambda\mathbf{I}-\mathbf{Q}_{m+1}^+\cfrac{\mathbf{I}}{\mathbf{Q}_{m+2}+\lambda\mathbf{I}-\cdots}\mathbf{Q}_{m+2}^-}\mathbf{Q}_{m+1}^-}\mathbf{Q}_m^-\ . \tag{5.5}$$

For $m=0$ (4.13) reduces to

$$\mathbf{K}(\lambda)\hat{\mathbf{c}}_0=[\mathbf{Q}_0^+\mathbf{S}_1+\mathbf{Q}_0+\lambda\mathbf{I}]\hat{\mathbf{c}}_0=0\ . \tag{5.6}$$

Equation (5.6) has only a nontrivial solution if the determinant of $\mathbf{K}(\lambda)$ vanishes, i.e.,

$$\det(\lambda)=\det[\mathbf{K}(\lambda)]=0\ . \tag{5.7}$$

This condition determines the eigenvalues of (4.13), or equivalently (4.2), (3.12), and (2.2). It should be noted that from the structure of the matrices $\mathbf{Q}_m^\pm$ and $\mathbf{Q}_m$ one can conclude that for $\lambda=0$ the first line of the truncated matrix $\mathbf{K}(0)$ only consists of zeros. Therefore the untruncated system (4.13) as well as the truncated system have a stationary solution.

The procedure for solving the vector recurrence relation (4.13) now runs as follows: We start with $\mathbf{S}_{M+1}=0$, yielding $\hat{\mathbf{c}}_{M+1}=0$ as required by (5.1), and calculate by iterative use of (5.4) the matrix $\mathbf{K}(\lambda)$ and its determinant $\det(\lambda)$. By a proper root-finding technique we find one of the eigenvalues λ. The eigenvalue $\lambda=0$ is already known and need not be determined in this way. With the known eigenvalue we then calculate the matrices $\mathbf{S}_M,\mathbf{S}_{M-1},\ldots,\mathbf{S}_2,\mathbf{S}_1$ according to (5.4) and solve (5.6) for $\hat{\mathbf{c}}_0$. Then the vectors $\hat{\mathbf{c}}_1,\hat{\mathbf{c}}_2,\ldots,\hat{\mathbf{c}}_M$ are obtained by repeatedly using (5.2), i.e., by

$$\hat{\mathbf{c}}_1=\mathbf{S}_1\hat{\mathbf{c}}_0,\quad\hat{\mathbf{c}}_2=\mathbf{S}_2\hat{\mathbf{c}}_1,\quad\hat{\mathbf{c}}_3=\mathbf{S}_3\hat{\mathbf{c}}_2,\ldots\ . \tag{5.8}$$

The eigenfunctions and the stationary solution finally follow by using (4.9) and performing the summation in (4.3) truncated at $m=M$ and $n=N$. The iteration according to (5.8) is numerically stable, whereas the iteration of (4.13) starting with $\hat{\mathbf{c}}_0$ and $\hat{\mathbf{c}}_1=\mathbf{S}_1\hat{\mathbf{c}}_0$ is numerically unstable.[20]

VI. RESULTS

First we discuss some stationary Q functions. We have chosen $\Omega/\chi=10$, i.e., an integer value. For $\Omega/\chi=9.5$ (not shown here) the situation is quite similar, except that the transition field for small κ is not as low as it is for $\Omega/\kappa=10$. Because the number of thermal photons at room temperature is negligible for optical frequencies, we mainly restrict our calculations to $n_{\rm th}=0$. The cavity damping constants are $\kappa=0.001\Omega$ (Fig. 2) and $\kappa=0.1\Omega$ (Fig. 3). Figures 2(a) and 3(a) show the Q functions for small driving fields. They have only one maximum and no bistability occurs. The lines $Q=$const have a circular shape. In Figs. 2(b) and 3(b) the driving field is large enough to allow two maxima for the Q function. From the two maxima one can conclude that the system is bistable for these driving fields. If the driving field is increased further the left maximum of the Q function disappears [see Figs. 2(c) and 3(c)] and only one ear-shaped distribution remains, indicating that the system is no longer bistable. Comparing Fig. 2 and Fig. 3 one realizes that the influence of κ is twofold. For small cavity damping ($\kappa=0.001\Omega$) the Q functions are almost symmetric with respect to the real axis. For higher cavity damping the Q functions seem to be rotated. Furthermore, the field at which the system is bistable is shifted to lower driving fields if κ is decreased. (For $\Omega/\chi=9.5$ the influence of κ on the shifts of the driving fields is much

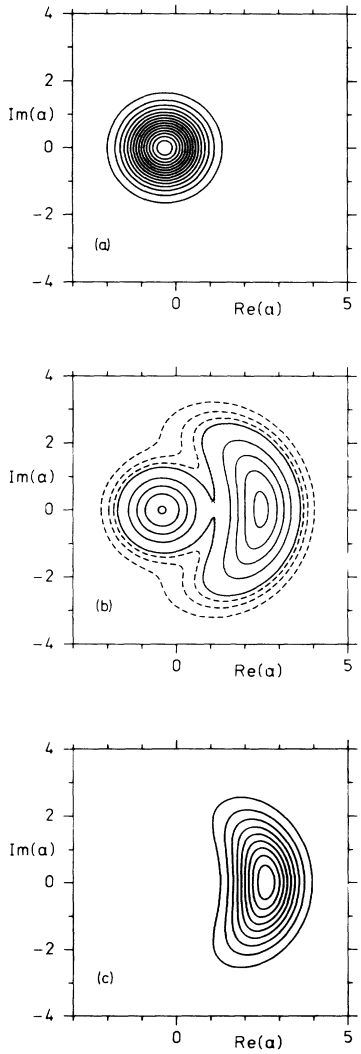

FIG. 2. Contour lines of the stationary Q function for $\Omega/\chi=10$, $n_{\rm th}=0$, and $\kappa/\Omega=0.001$. The normalized driving fields $\bar{F}$ are (a) 0.1, (b) 0.125, and (c) 0.25. The solid lines represent $Q=0.02$, 0.04, 0.06, ..., the dashed lines in (b) $Q=0.005$, 0.010, and 0.015. The contour line through the saddle point (dotted line) is at $Q=0.0201$.

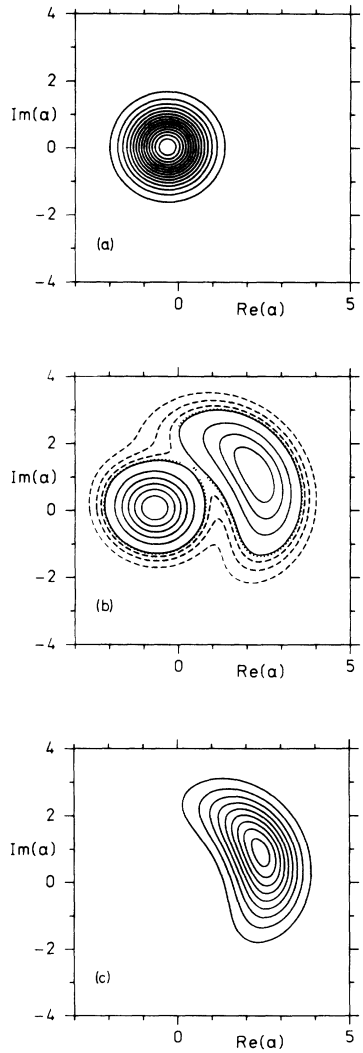

FIG. 3. Contour lines of the stationary Q function for $\Omega/\chi=10$, $n_{\rm th}=0$, and $\kappa/\Omega=0.1$. The normalized driving fields $\bar{F}$ are (a) 0.1, (b) 0.195, and (c) 0.25. The solid lines represent $Q=0.02$, 0.04, 0.06, ..., the dashed lines in (b) $Q=0.005$, 0.010, and 0.015. The contour line through the saddle point (dotted line) is at $Q=0.0187$.

weaker; see the discussion of the tunneling rates below.) Note that the Q functions do not get broader for higher damping constants. We want to emphasize that the Q functions have been obtained via a pseudo-Fokker-Planck equation with a non-positive-definite diffusion matrix and nonlinear drift coefficients. As one can clearly see in Fig. 2 and Fig. 3 the Q functions are well behaved and no singularities occur.

Due to squeezing the P function does not exist in general. The expansion coefficients, however, are connected to the mean values [see (4.8)] and do exist. But if one tries to evaluate the sum (4.3) for the P function the result oscillates and depends on the scaling intensity I_s as well as on the truncation indices N and M. In order to demonstrate this behavior we have plotted in Fig. 4 the sum (4.3) for the stationary case (a) for the Q function and (b) for the P function along the real axis for various truncation indices N and M using the parameters of Fig. 3(b) (for these parameters bistability occurs). The scaling intensity is $I_s=1.5$ for the Q function and $I_s=0.5$ for the P function (which was a good choice for calculating mean values and eigenvalues). As can be seen the sum (4.3) converges for the Q function, whereas it does not converge for the P function. For the P function the result oscillates and becomes larger if more terms are taken into account. If the number of terms is further increased numerical overflows occur and the sum cannot be evaluated numerically anymore.

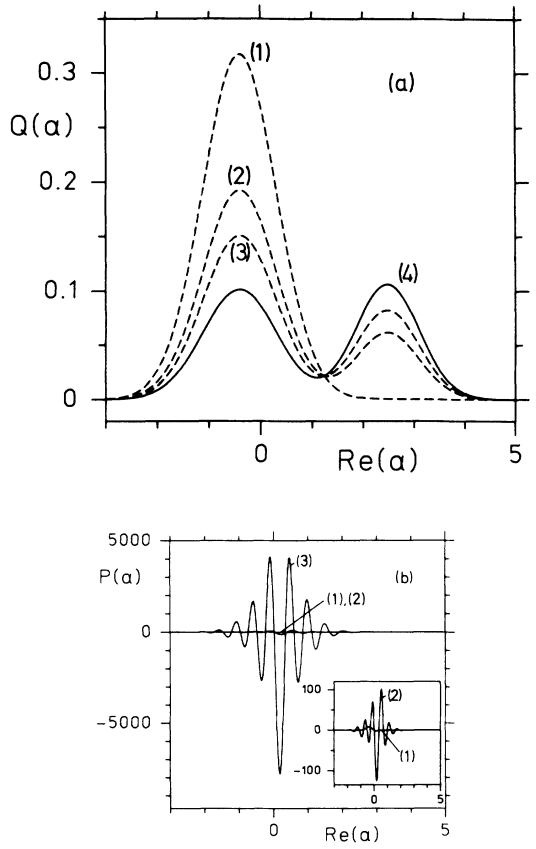

FIG. 4. Cross section of the truncated sum (4.3) for (a) the Q function and (b) the P function along the real axis for various truncation indices. The parameters are those of Fig. 2(b). The sum for the (a) Q function is truncated at (1) $N=5$, $M=10$, (2) $N=10$, $M=20$, and (3) $N=14$, $M=50$. Curve (4) shows the limit $N\to\infty$, $M\to\infty$ calculated with $N=20$, $M=120$. The sum for the P function is truncated at (1) $N=5$, $M=10$, (2) $N=7$, $M=15$, and (3) $N=10$, $M=20$. The inset shows curve (1) and (2) in an enlarged scale. The limit $N\to\infty$, $M\to\infty$ does not exist.

In Ref. 37 a nonlinear Kerr medium was investigated. It is interesting to notice that our ear-shaped Q functions in Figs. 2(c) and 3(c) and the right part of our Q functions in Figs. 2(b) and 3(b) are similar to the Q functions generated by a nonlinear Mach-Zehnder interferometer,[37] which have been called crescent shaped. In Ref. 37 it is shown that these Q functions describe number-phase minimum-uncertainty states. The nonlinear Kerr medium inside the interferometer is described by the operator $a^{\dagger 2}a^2$ also occurring in our Hamiltonian (2.3).

In Fig. 5 the stationary mean value $\langle a\rangle$ for $n_{\rm th}=0$ is shown for different values of κ. (The variances of the quadrature phases can also be calculated. As shown in Ref. 22 slightly squeezed states exist for driving fields above the bistable region.) Our results agree with the result obtained by Drummond and Walls[5] using the complex P representation. In this representation detailed balance is valid for $n_{\rm th}=0$. Therefore an analytical expression $\langle a^{\dagger n}a^m\rangle$ could be derived. With the abbreviations

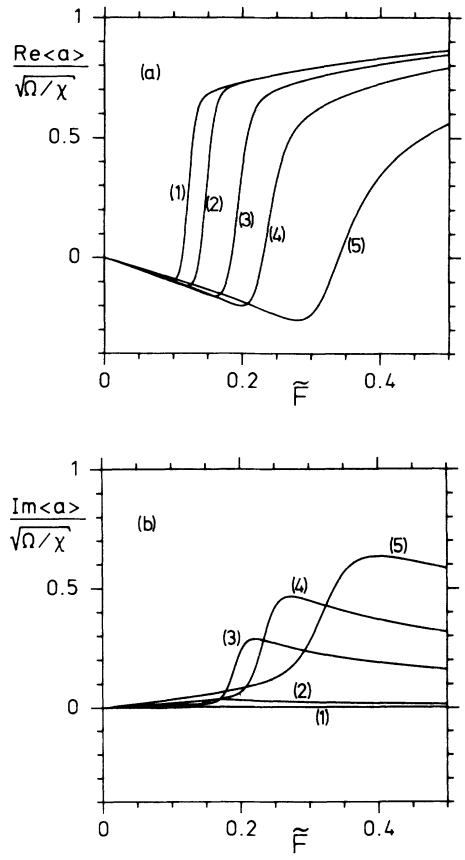

FIG. 5. (a) Real part and (b) imaginary part of the stationary expectation value $\langle a\rangle$ as a function of the normalized driving field $\tilde{F}$ for $\Omega/\chi=10$ and $n_{\rm th}=0$. The cavity damping constants κ/Ω are (1) 0.001, (2) 0.01, (3) 0.1, (4) 0.2, and (5) 0.4.

$$c=-\Omega/\chi-i\kappa/\chi,\quad z=2(F/\chi)^2\ , \tag{6.1}$$

their result reads

$$\langle a^{\dagger n}a^m\rangle=\left[\frac{z}{2}\right]^{(n+m)/2}\frac{\Gamma(c)\Gamma(c^*)}{\Gamma(c+m)\Gamma(c^*+n)}\times\frac{{}_0F_2(c+m,c^*+n,z)}{{}_0F_2(c,c^*,z)}\ . \tag{6.2}$$

Here Γ is the gamma function and ${}_0F_2$ is the generalized Gauss hypergeometric series.[34,38] Because detailed balance is essential for the derivation of (6.2) no analytical expression for the mean values can be obtained by the method used in Ref. 5 for $n_{\rm th}>0$. Our method, however, is also applicable for $n_{\rm th}>0$. Just to demonstrate that it also works in the presence of thermal fluctuations, some results for $n_{\rm th}=0.5$ are shown in Fig. 6. (Though $n_{\rm th}=0.5$ is much too large for optical photons at room temperatures the model may also be applied to dispersive bistability for microwaves. In such a system the number of thermal quanta is of the order of unity or even larger.)

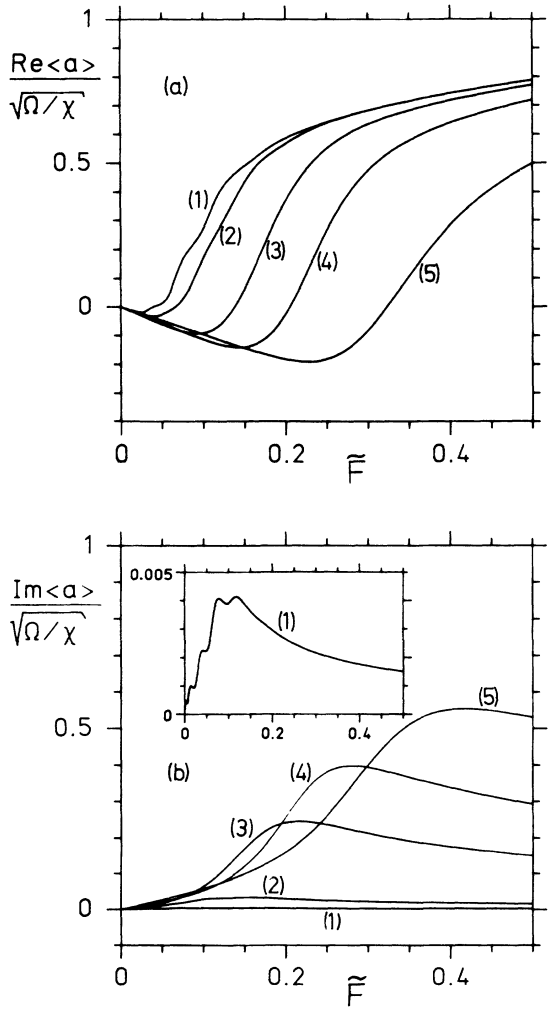

FIG. 6. Same as Fig. 5 but for $n_{\rm th}=0.5$. The inset in (b) shows the imaginary part of $\langle a\rangle$ for $\kappa=0.001\Omega$ in an enlarged scale.

For $\kappa=0.001\Omega$ small ripples appear for the expectation value $\langle a\rangle$ in the left part of the figure which do not occur for $n_{\rm th}=0$. We would like to point out that in the lowest nonzero eigenvalue of Fig. 7(b) a similar ripple structure occurs, though not as pronounced as in Fig. 6(b). For noninteger Ω/χ values or for larger damping constants this ripple structure disappears.

Next we discuss the results for the eigenvalues of equation (4.2), i.e., we look for nonzero λ's satisfying (5.7). Because $n_{\rm th}$ is very small for optical photons we confine ourselves to the case $n_{\rm th}=0$ (pure quantum noise). Some of the lowest real eigenvalues for small ($\kappa=0.001\Omega$) and larger ($\kappa=0.1\Omega$) damping constants are shown in Figs. 7 and 8 for (a) $\Omega/\chi=9.5$ and (b) $\Omega/\chi=10$. It can be shown that for zero driving fields the eigenvalues of (4.2) are $0,2\kappa,4\kappa,6\kappa,\ldots$. Therefore we have plotted the eigenvalues divided by 2κ. Furthermore, we want to emphasize that the eigenvalues obtained from the Q function and those obtained from the P function agree within the numerical accuracy. As already mentioned, the problem of representation-dependent results does not arise in our calculations. For $\Omega/\chi=9.5$ and $\kappa=0.001\Omega$ our results agree with the results obtained from the procedure used in Ref. 10 for the small-damping limit. For integer Ω/χ values, however, the procedure used in Ref. 10 does not work.

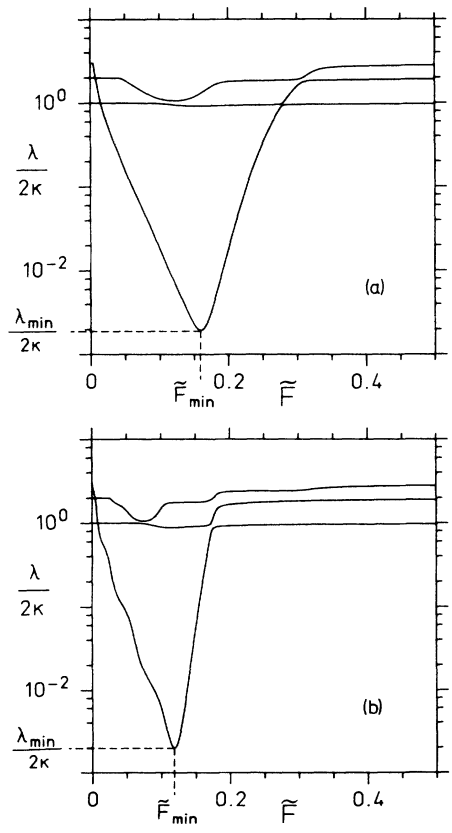

FIG. 7. Plot of the first three nonvanishing real eigenvalues in a logarithmic scale as a function of the normalized driving field $\tilde{F}$ for $\kappa=0.001\Omega$ and $n_{\rm th}=0$. The values for Ω/χ are (a) 9.5 and (b) 10.

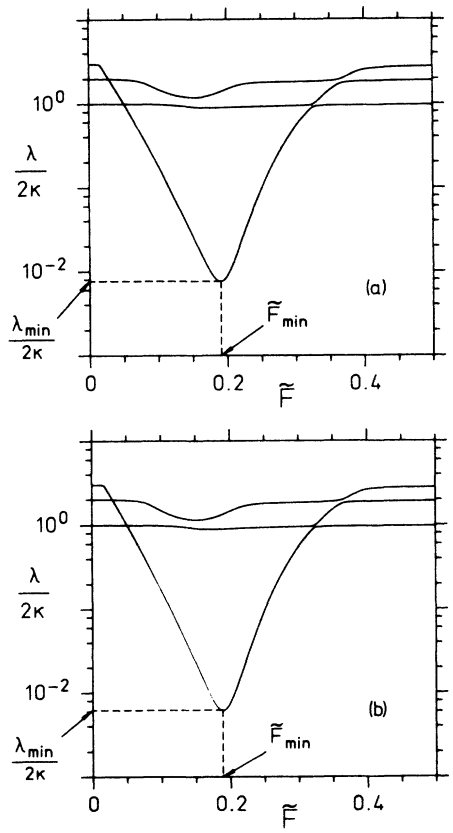

FIG. 8. Same as Fig. 7 but for $\kappa=0.1\Omega$.

For driving fields allowing bistability, the lowest nonzero eigenvalue is well separated from the higher eigenvalues and therefore determines the long-time behavior of the system. An eigenfunction (Q function) corresponding to the lowest nonzero eigenvalue for a driving field which allows bistability is shown in Fig. 9. By comparing this figure to Figs. 2(b) and 3(b) (note the positive sign of the stationary Q function and the different signs of the eigenfunction of Fig. 9) we conclude that the lowest nonzero eigenvalue and the corresponding eigenfunction describe transitions between the two almost-stable states of our bistable system, i.e., the tunneling rate is determined by the lowest nonzero eigenvalue. Because we have neglected thermal fluctuations this eigenvalue determines the ultimate stability of our system, as already mentioned in the Introduction.

For $\kappa=0.1\Omega$ the results for $\Omega/\chi=9.5$ and $\Omega/\chi=10$ do not differ very much (see Fig. 8). For $\kappa=0.001\Omega$, however, ripples occur for integer Ω/χ values, whereas for noninteger Ω/χ values these ripples disappear. Furthermore, the driving field $\tilde{F}_{min}$, where the lowest nonzero eigenvalue has its minimum λ_{min}, changes appreciably if the parameter Ω/χ is slightly increased from 9.5 to 10.0 (see Fig. 7). In order to show this behavior more clearly we plotted the driving field $\tilde{F}_{min}$ and the corresponding eigenvalue λ_{min} as a function of the parameter Ω/χ. The results are shown in Fig. 10. For small cavity damping ($\kappa=0.001\Omega$) one can clearly see that the field $\tilde{F}_{min}$ reaches very low values at integer values of Ω/χ and increases very sharply when moving away from integer values. For large Ω/χ values this oscillating behavior is less pronounced. The minimum eigenvalue corresponding to $\tilde{F}_{min}$ decreases roughly exponentially if Ω/χ is increased. At integer values of Ω/χ, however, the eigenvalue has peaks leading to somewhat larger values at and near integer values for Ω/χ. For small Ω/χ values the first nonvanishing eigenvalue is no longer well separated

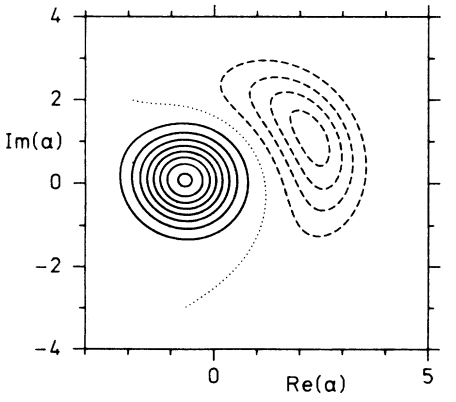

FIG. 9. Contour lines of the eigenfunction corresponding to the lowest nonvanishing eigenvalue for the parameters of Fig. 3(b). The solid lines and the dashed lines indicate the different sign of the eigenfunction. The dotted line represents $Q=0$.

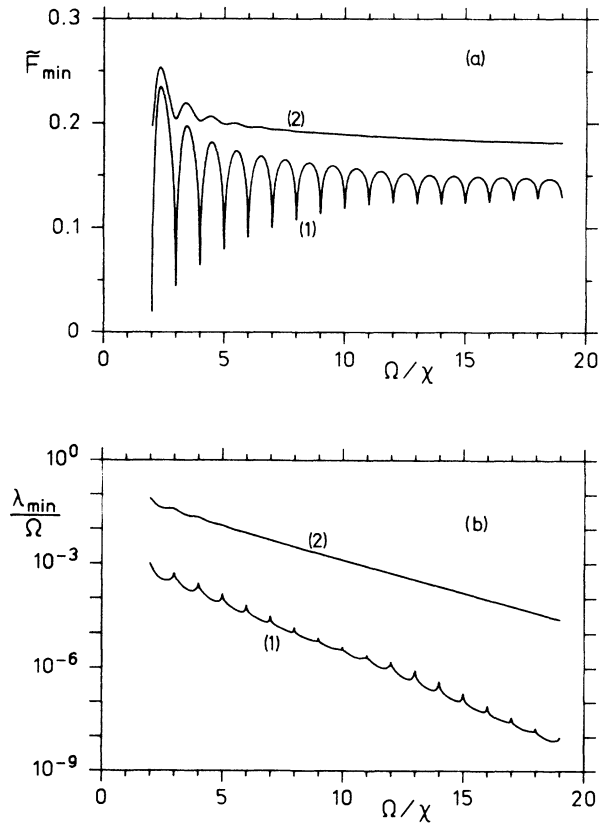

FIG. 10. (a) The normalized driving field $\tilde{F}_{min}$, where the lowest eigenvalue has its minimum and (b) the corresponding minimum eigenvalue (see Figs. 7 and 8) as a function of Ω/χ for (1) $\kappa=0.001\Omega$ and (2) $\kappa=0.1\Omega$.

from the higher eigenvalues even in the bistable region (the higher eigenvalues are of the order 2κ). Therefore we did not investigate $\Omega/\chi<2$. For larger damping constants the results for integer Ω/χ no longer differ appreciably from the results for noninteger Ω/χ values. For small cavity damping and Ω/χ values which are not too large we have therefore the following result: At integer Ω/χ values the bistable region is appreciably shifted towards smaller driving fields and the tunneling rate itself increases, i.e., the system becomes less stable. It can be shown[39] that this remarkable result for integer Ω/χ values at small damping constants is due to the fact that for integer Ω/χ values some of the lower eigenvalues of the Hamiltonian (2.3) are exactly degenerate for $F=0$ and remain almost degenerate for finite driving fields. A detailed investigation for small damping constants including the differences between integer and noninteger Ω/χ values are discussed in Ref. 39, where an approximation for small cavity damping is presented. In contrast to the approximation made in Ref. 10, which was not valid for integer or near-integer values of Ω/χ, it is applicable for arbitrary parameters Ω/χ. (In addition to the procedure in Ref. 10, where only diagonal elements of the density operator have been taken into account, some appropriate nondiagonal elements must be included for integer or near-integer values of Ω/χ.)

VII. CONCLUSION

We have calculated quantum-tunneling rates and the stationary Q functions for the model of Drummond and Walls describing dispersive optical bistability by solving a pseudo-Fokker-Planck equation with the matrix continued-fraction method. We have shown that the stationary Q function is well behaved although the diffusion matrix of the pseudo-Fokker-Planck equation is not positive definite. Generally, the P function does not exist. Nevertheless, we have demonstrated that its equation of motion can be used for calculating expectation values and eigenvalues. The expectation values and eigenvalues obtained from the P function agree very accurately with those obtained from the Q function. The investigation of tunneling rates was one important feature of our calculations. In the bistable region the lowest nonzero eigenvalue is well separated from the higher ones and therefore describes the decay rate of the two almost-stable states. Although it may become very small it can be calculated with high precision by the matrix continued-fraction method. We have found that for small cavity damping constants the driving field, where the tunneling rate has its minimum, varies appreciably in an oscillating fashion as a function of the parameter Ω/χ. Due to the quantum nature of the problem the system behaves different for integer and noninteger Ω/χ values if the cavity damping is small enough. The main effect of integer Ω/χ values is an appreciable shift of the bistable region towards lower driving fields.

As an extension to the calculations presented here, we hope that time-dependent correlation functions can also be obtained by the matrix continued-fraction method. An application of this method to more complicated problems seems also to be feasible. If, for instance, we consider a single light mode coupled to a two-level atom, (Jaynes-Cummings model[40]) the density operator elements ρ_{ij} of the two-level system, which are still operators with respect to the light mode, can also be transformed to continuous functions with one complex variable. An expansion of these functions as well as a transformation to a tridiagonal vector recurrence relation and a solution by MCF's seems to be possible.

Note added in proof. Recently the equation of motion for the Wigner function (3.13) was also solved by the matrix continued-fraction method.[41] The work of Lugiato and co-workers[42] should also be mentioned. For optical bistability they found a Fokker-Planck equation for the P function with a non-positive-definite diffusion matrix. By using a linearization procedure they also found a slight amount of squeezing.

APPENDIX: SIMPLE EXAMPLE OF A FOKKER-PLANCK-LIKE EQUATION WITH NONPOSITIVE DIFFUSION MATRIX

In this appendix we show that Fokker-Planck-like equations with a non-positive-definite diffusion matrix can have nonsingular solutions. Such equations are already discussed in Refs. 15 and 16, but no well-behaved (quasi)distribution functions are obtained in these references. A simple Fokker-Planck-like equation with a non-positive-definite diffusion matrix is given in the following ($q>0$):

$$\frac{\partial P}{\partial t}=\left[\frac{\partial}{\partial x}(x-\omega y)+\frac{\partial}{\partial y}(y+\omega x)+\frac{\partial^2}{\partial x^2}-q\frac{\partial^2}{\partial y^2}\right]P\ . \tag{A1}$$

The drift term describes a damped rotation according to the deterministic equations

$$\dot{x}=-x+\omega y,\quad \dot{y}=-y-\omega x\ . \tag{A2}$$

The Fourier transform of (A1) reads

$$\frac{\partial\tilde{P}}{\partial t}=-\left[(k_1+\omega k_2)\frac{\partial}{\partial k_1}+(k_2-\omega k_1)\frac{\partial}{\partial k_2}+k_1^2-qk_2^2\right]\tilde{P}\ , \tag{A3}$$

where P is defined by

$$\tilde{P}(k_1,k_2,t)=\int P(x,y,t)e^{-ik_1x-ik_2y}dx\,dy\ . \tag{A4}$$

If the initial distribution function $P(x,y,t=0)$ is Gaussian the Fourier transform $\tilde{P}(k_1,k_2,t=0)$ is Gaussian, too. Because of the form of (A3) we expect that $\tilde{P}$ is Gaussian for $t>0$ and make the ansatz

$$\tilde{P}(k_1,k_2,t)=\exp[-iM_1(t)k_1-iM_2(t)k_2-\tfrac{1}{2}\sigma_{11}(t)k_1^2-\sigma_{12}(t)k_1k_2-\tfrac{1}{2}\sigma_{22}(t)k_2^2]\ . \tag{A5}$$

The prefactor 1 in the exponential function is a consequence of the normalization

$$\int P(x,y,t)dx\,dy=1\ , \tag{A6}$$

which requires

$$\tilde{P}(k_1=0,\ k_2=0,\ t)=1\ . \tag{A7}$$

Substituting the ansatz (A5) into (A3) yields the following ordinary differential equations for M_1 and M_2 and σ_{11}, σ_{12}, and σ_{22}:

$$\dot{M}_1=-M_1+\omega M_2,\quad \dot{M}_2=-\omega M_1-M_2\ , \tag{A8}$$

$$\dot{\sigma}_{11}=-2\sigma_{11}+2\omega\sigma_{12}+2\ ,$$

$$\dot{\sigma}_{12}=-2\sigma_{12}+\omega(\sigma_{22}-\sigma_{11})\ , \tag{A9}$$

$$\dot{\sigma}_{22}=-2\sigma_{22}-2\omega\sigma_{12}-2q\ .$$

Defining the matrices $\boldsymbol{\sigma}$ and $\mathbf{U}$ by

$$\boldsymbol{\sigma}=\begin{bmatrix}\sigma_{11} & \sigma_{12}\\ \sigma_{12} & \sigma_{22}\end{bmatrix},\quad \mathbf{U}=\begin{bmatrix}\cos(\omega t) & \sin(\omega t)\\ -\sin(\omega t) & \cos(\omega t)\end{bmatrix} \tag{A10}$$

and the vector $\mathbf{M}$ by

$$\mathbf{M}=\begin{bmatrix}M_1\\ M_2\end{bmatrix}\ , \tag{A11}$$

the time-dependent solution to (A8) and (A9) reads

$$\mathbf{M}(t)=e^{-t}\mathbf{U}(t)\mathbf{M}(0)\ , \tag{A12}$$

$$\boldsymbol{\sigma}(t)=\boldsymbol{\sigma}(\infty)-e^{-2t}\mathbf{U}(t)[\boldsymbol{\sigma}(\infty)-\boldsymbol{\sigma}(0)]\mathbf{U}^T(t)\ , \tag{A13}$$

where the vector $\mathbf{M}(0)$ and the matrix $\boldsymbol{\sigma}(0)$ follows from the special form of the initial Gaussian function and where $\boldsymbol{\sigma}(\infty)$ is the stationary solution of (A9) given by

$$\sigma_{11}(\infty)=\frac{1}{2}\left[1-q+\frac{1+q}{1+\omega^2}\right]\ ,$$

$$\sigma_{12}(\infty)=-\frac{\omega}{2}\frac{1+q}{1+\omega^2}\ , \tag{A14}$$

$$\sigma_{22}(\infty)=\frac{1}{2}\left[1-q-\frac{1+q}{1+\omega^2}\right]\ .$$

If the matrix $\boldsymbol{\sigma}(t)$ is positive definite for $t\geq 0$, $\tilde{P}(k_1,k_2,t)$ is Gaussian and therefore its Fourier transform, i.e., $P(x,y,t)$ is Gaussian, too. However, if $\boldsymbol{\sigma}(t)$ is not positive definite for $t\geq 0$ the Fourier transform $P(x,y,t)$ of $\tilde{P}(k_1,k_2,t)$ does not exist. The matrix $\boldsymbol{\sigma}$ is positive definite if

$$\sigma_{11}>0,\quad \sigma_{22}>0,\quad \sigma_{11}\sigma_{22}-\sigma_{12}\sigma_{12}>0\ . \tag{A15}$$

From these conditions it follows that the stationary solution $\boldsymbol{\sigma}(\infty)$ is positive definite for

$$q<1,\quad 1+\omega^2>(1+q)^2/(1-q)^2\ . \tag{A16}$$

Note that these conditions do not depend on the special form of the initial Gaussian distribution function.

For the time-dependent matrix $\boldsymbol{\sigma}(t)$ the conditions (A15) are more difficult to handle. Therefore we restrict ourselves to some numerical examples, i.e., diagonalize $\boldsymbol{\sigma}(t)$ numerically. The matrix $\boldsymbol{\sigma}$ is positive definite if both eigenvalues (σ_1 and σ_2) of $\boldsymbol{\sigma}$ are positive. If at least one of its eigenvalues is negative, $\tilde{P}$ diverges for large k_1, k_2 and thus $P(x,y,t)$ will no longer exist. If we start with an initially positive definite matrix $\boldsymbol{\sigma}(0)$ there are three typical cases which are shown in Fig. 11. (1) The lower eigenvalue of $\boldsymbol{\sigma}(t)$ becomes negative and remains negative for $t\to\infty$ [see curve (1)]. This means that the initially nonsingular distribution function $P(x,y,t=0)$ becomes singular and remains singular. (2) The lower eigenvalue of $\boldsymbol{\sigma}(t)$ first becomes negative and then becomes positive again [see curve (2)], i.e., the initially nonsingular distribution function first becomes singular and then becomes nonsingular again and stays this way for all larger t. (3) The lower eigenvalue of $\boldsymbol{\sigma}(t)$ is positive for all times [see curve (3)], i.e., the distribution function $P(x,y,t)$ is nonsingular for $t\geq 0$.

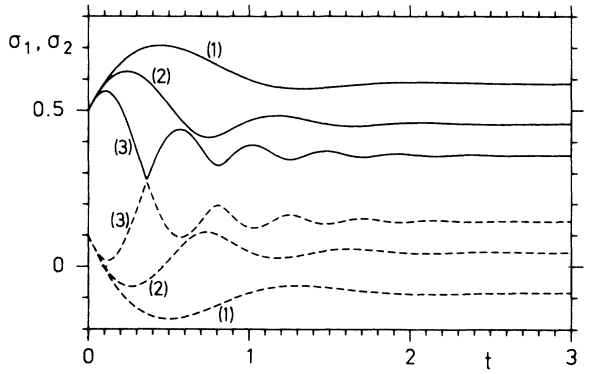

FIG. 11. The upper eigenvalue (solid lines) and the lower eigenvalue (dashed lines) of the matrix $\boldsymbol{\sigma}(t)$ as a function of time for $q=0.5$ and (1) $\omega=2$, (2) $\omega=3.5$, and (3) $\omega=7$. The initial matrix $\boldsymbol{\sigma}(0)$ is given by $\sigma_{11}(0)=0.5$, $\sigma_{22}(0)=0.1$, and $\sigma_{12}(0)=\sigma_{21}(0)=0$; $\boldsymbol{\sigma}$, t, q, and ω are dimensionless quantities.

The behavior of the solutions can be visualized by transforming (A1) to a reference system rotating with the angular velocity ω, i.e.,

$$x'=x\cos(\omega t)-y\sin(\omega t)\ ,$$
$$y'=x\sin(\omega t)+y\cos(\omega t)\ . \tag{A17}$$

This transformation yields

$$\frac{\partial P}{\partial t}=\left\{\frac{\partial}{\partial x'}x'+\frac{\partial}{\partial y'}y'+[\cos^2(\omega t)-q\sin^2(\omega t)]\frac{\partial^2}{\partial x'^2}\right.$$
$$+2(1+q)\sin(\omega t)\cos(\omega t)\frac{\partial^2}{\partial x'\partial y'}$$
$$\left.+[\sin^2(\omega t)-q\cos^2(\omega t)]\frac{\partial^2}{\partial y'^2}\right\}P\ . \tag{A18}$$

Since such a transformation does not alter the eigenvalues of the diffusion matrix, (A18) still has a non-positive-definite diffusion matrix which, in contrast to (A1), now depends on the time. If the rotation rate is much faster than the diffusion rate and the initial distribution is broad enough, we may perform a time average of the diffusion matrix and obtain

$$\bar{D}_{11}=\bar{D}_{22}=(1-q)/2, \quad \bar{D}_{12}=0 . \tag{A19}$$

This matrix is clearly positive definite for $q<1$. In order to obtain a nonsingular distribution the following three conditions must hold.

(1) $q<1$,
(2) ω is large enough,
(3) the initial distribution is broad enough.

The first two conditions are essentially the same as (A16). As a remark to the third condition we would like to mention that in quantum optics the Heisenberg uncertainty relation must be valid. In order to avoid a contradiction to that relation the Q function must be broad enough. Therefore we cannot start with initial conditions such as $P(x,y,t=0)=\delta(x-x_0)\delta(y-y_0)$ as one does when solving ordinary Fokker-Planck equations describing, for instance, a Brownian motion process where all particles start at $x=x_0$ and $y=y_0$.

In conclusion, we have shown for a Fokker-Planck-like equation with a linear drift term and a constant but not positive-definite diffusion matrix that a pseudo-Fokker-Planck equation need not necessarily have a positive definite or positive semidefinite diffusion matrix in order to have nonsingular solutions. As one can see in (A16) or in the conditions necessary for performing the time average, the ω terms in the drift terms of (A1) play an essential role for the existence of a nonsingular solution. Such "rotation terms" also occur in our equations (3.12) and (3.17).

[1] *Optical Bistability,* edited by C. M. Bowden, M. Cliftan, and H. R. Robl (Plenum, New York, 1981).
[2] *Dissipative Systems in Quantum Optics,* Vol. 27 of *Topics in Current Physics,* edited by R. Bonifacio (Springer, Berlin, 1982).
[3] L. A. Lugiato, in *Progress in Optics XXI,* edited by E. Wolf (North-Holland, Amsterdam, 1984), p. 69.
[4] J. C. Englund, R. R. Snapp, and W. C. Schieve, *Progress in Optics XXI,* edited by E. Wolf (North-Holland, Amsterdam, 1984), p. 355.
[5] P. D. Drummond and D. F. Walls, J. Phys. A **13**, 725 (1980).
[6] C. M. Savage and D. F. Walls, Phys. Rev. Lett. **57**, 2164 (1986).
[7] P. D. Drummond and C. W. Gardiner, J. Phys. A **13**, 2353 (1980).
[8] P. D. Drummond, C. W. Gardiner, and D. W. Walls, Phys. Rev. A **24**, 914 (1981).
[9] C. W. Gardiner, *Handbook of Stochastic Methods,* Vol. 13 of *Springer Series in Synergetics* (Springer, Berlin, 1985).
[10] H. Risken, C. Savage, F. Haake, and D. F. Walls, Phys. Rev. A **35**, 1729 (1987).
[11] R. J. Glauber, Phys. Rev. Lett. **10**, 84 (1963); Phys. Rev. **131**, 2766 (1963).
[12] E. C. G. Sudarshan, Phys. Rev. Lett. **10**, 277 (1963).
[13] E. Wigner, Phys. Rev. **40**, 749 (1932).
[14] M. Hillery, R. F. O'Connell, M. O. Scully, and E. P. Wigner, Phys. Rep. **106**, 121 (1984).
[15] H. P. Yuen and P. Tombesi, Opt. Commun. **59**, 155 (1986).
[16] W. Tan, Y. Li, and W. Zhang, Opt. Commun. **64**, 195 (1987).
[17] H. J. Carmichael and M. Wolinsky, in *Quantum Optics IV,* edited by J. D. Harvey and D. F. Walls (Springer, Berlin, 1986), p. 208.
[18] M. Dörfle and A. Schenzle, Z. Phys. B **65**, 113 (1986).
[19] H. Risken and H. D. Vollmer, Z. Phys. B **33**, 297 (1979); H. D. Vollmer and H. Risken, *ibid.* **34**, 313 (1979); Physica A **110**, 106 (1982); H. Risken and H. D. Vollmer, Mol. Phys. **46**, 555 (1982).
[20] H. Risken, *The Fokker-Planck Equation,* Vol. 18 of *Springer Series in Synergetics* (Springer, Berlin, 1984).
[21] K. Vogel and H. Risken, Opt. Commun. **62**, 45 (1987).
[22] H. Risken and K. Vogel, in *Fundamentals of Quantum Optics II,* edited by F. Ehlotzky (Springer, Berlin, 1987), p. 225.
[23] H. Risken and K. Vogel, in *Optical Bistability, Instability and Optical Computing,* edited by H.-Y. Zhang and K. K. Lee (World Scientific, Singapore, 1988), p. 136.
[24] P. D. Drummond and D. F. Walls, Phys. Rev. A **23**, 2563 (1981).
[25] C. M. Savage and H. J. Carmichael (unpublished).
[26] G. Duffing, *Erzwungene Schwingungen bei veränderlicher Eigenfrequenz und ihre technische Bedeutung* (Vieweg, Braunschweig, 1918).
[27] A. H. Nayfeh and D. T. Mook, *Nonlinear Oscillations* (Wiley, New York, 1979), p. 162ff.
[28] H. Haken, in *Laser Theory,* Vol. XXV/2c of *Encyclopedia of Physics,* edited by S. Flügge (Springer, Berlin, 1970).
[29] W. L. Louisell, *Quantum Statistical Properties of Radiation* (Wiley, New York, 1973).
[30] D. F. Walls, Nature **306**, 141 (1983).
[31] P. D. Drummond, Phys. Rev. A **33**, 4462 (1986).
[32] R. Graham and A. Schenzle, Phys. Rev. A **23**, 1302 (1981).
[33] H. Haug, S. W. Koch, R. Neumann, and H. E. Schmidt, Z. Phys. B **49**, 79 (1982).
[34] W. Magnus, F. Oberhettinger, and R. P. Soni, *Formulas and Theorems for the Special Functions of Mathematical Physics* (Springer, Berlin, 1966).
[35] H. Risken and H. D. Vollmer, Z. Phys. B **39**, 89 (1980); **39**, 339 (1980).
[36] H. E. Stanley, *Introduction to Phase Transitions and Critical Phenomena* (Clarendon, Oxford, 1971).
[37] M. Kitagawa and Y. Yamamoto, Phys. Rev. A **34**, 3974 (1986).
[38] I. S. Gradshteyn and I. M. Ryzhik, *Table of Integrals Series and Products,* 4th ed. (Academic, New York, 1965).
[39] H. Risken and K. Vogel, Phys. Rev. A **38**, 1349 (1988).
[40] E. T. Jaynes and F. W. Cummings, Proc. IEEE **51**, 89 (1963).
[41] K. Vogel and H. Risken (unpublished).
[42] M. Gronchi and L. A. Lugiato, Lett. Nuovo Cimento **23**, 593 (1978); L. A. Lugiato and G. Strini, Opt. Commun. **41**, 67 (1982).